

## REUSE OF EXPIRED CEFORT DRUG IN NICKEL ELECTRODEPOSITION FROM WATTS BATH

Delia-Andrada Duca, Mircea Laurentiu Dan, Nicolae Vaszilcsin \*

Faculty of Industrial Chemistry and Environmental Engineering, University Politehnica Timisoara,  
6, V. Parvan Blvd., Timisoara 300223, Romania

\*e-mail: nicolae.vaszilcsin@upt.ro; phone: (+40) 256 406 180; fax: (+40) 256 403 060

**Abstract.** In this paper, the possibility to use ceftriaxone (CEFTR) active compound from expired Cefort<sup>®</sup> drug as additive in nickel electrodeposition from Watts bath has been investigated. Electrochemical behaviour of CEFTR and preliminary information about its influence on nickel electrodeposition process were obtained using cyclic voltammetry technique. Cyclic voltammograms have been drawn on platinum electrode at scan rates between 5 and 500 mV s<sup>-1</sup>. Linear voltammograms recorded at low scan rate emphasized the influence of the drug concentration in 5 g L<sup>-1</sup> Ni<sup>2+</sup> electrolyte solution. Kinetic parameters such as exchange current density and cathodic transfer coefficient have been calculated using Tafel polarization plots at different temperatures in the range of 25÷65°C. Further, activation energy has been determined from Arrhenius plots. Electrochemical impedance spectroscopy technique was used to study the charge transfer resistance and surface coverage degree in the same solutions at different deposition potentials.

**Keywords:** expired Cefort<sup>®</sup> drug, electroplating additive, nickel electrodeposition, Watts bath.

Received: 30 March 2017/ Revised final: 28 April 2017/ Accepted: 02 May 2017

---

### Introduction

Although known for over a century, nickel and nickel alloys electrodeposition currently maintain their utility due to the various applications in branches of modern industry as automotive, computer circuits, *etc.* [1,2]. The wide use of nickel deposits is based on both decorative qualities and anticorrosion properties of the metal layers even in strong aggressive media (H<sub>2</sub>SO<sub>4</sub>, HCl, NaCl solutions) [3-5].

Known as the most effective nickel deposition solution, Watts bath is characterized by its simplicity as well as its long time stability and low toxicity. In order to obtain high quality nickel layers, besides the basic components (NiSO<sub>4</sub>·7H<sub>2</sub>O, NiCl<sub>2</sub>·6H<sub>2</sub>O and H<sub>3</sub>BO<sub>3</sub>), levelling, brightening and anti-pitting agents must be added [6].

Current research in this area is focused on finding new compounds, cheaper than the existing ones, possibly by recycling of non-compliant substances from areas, for which they were initially designed for, but having the same behaviour as the well-known additives.

Watts baths have a high throwing power even without additives, the reason why the current density is constant on both the micropeaks and microgrooves. In these circumstances, the

deposited nickel layer is not able to cover the tiny cracks and defects onto the substrate surface. In order to obtain uniform deposits of nickel from Watts baths, addition of levelling and brightening agents is required [7-10]. As it is known, brighteners from primary and secondary class are used for mirror-bright ornamental nickel layers. Generally, Watts baths additives are organic compounds, which are preferentially adsorbed on the micropeaks. Therefore, the current density in these areas will decrease, while it will increase in microgrooves [11]. The presence of unsaturated bounds or aromatic structures in their molecules is the main characteristic of these additives. Such structural elements are also found in the active substances from drugs, therefore it is expected to have the same or similar effect as the traditional additives used in Watts baths [12].

The quantity of unused drugs for medical purpose daily increases mainly due to three reasons: exceeding the expiration date, non-compliant or counterfeit batches and discontinuation of patients treatment. A large part of them are incinerated, but it also remains an important quantity, which is eliminated in the residual water, thus polluting the environment [13,14]. To avoid the costs related to incineration or depollution, recycling of unused

drugs as additives in electroplating baths, Watts bath in the present case, is an alternative use [15].

The aim of this paper is to study CEFTR effect on nickel electrodeposition from Watts type bath due to the presence of nitrogen and sulphur heterocycles as well as C=C, C=O, C=N double bonds into its structure. Also, the heteroatoms with lone pair electrons are present in its molecule, making it able to be adsorbed on the metal surface. The object of this work involves as well the electrochemical behaviour of CEFTR, because of its interaction with the electrodes of the electrochemical cell.

## Experimental

Electrochemical experiments have been performed using a PARSTAT 2273 potentiostat/galvanostat in a 100mL thermostatted glass cell equipped with Pt and Ni working electrodes (0.8 cm<sup>2</sup> exposed area), two graphite rods counter electrodes, placed symmetrically to the working electrode and a Ag/AgCl reference electrode ( $E_{\text{Ag/AgCl}} = 0.197 \text{ V}$  vs normal hydrogen electrode). All further potentials are referred to this reference electrode.

Before starting each electrochemical measurement, platinum electrode was washed with distilled water and nickel electrode has been abraded with different grit emery papers, polished with polycrystalline diamond (6  $\mu\text{m}$ ), washed with distilled water and finally dried.

Electrochemical behaviour of CEFTR in 0.5 mol L<sup>-1</sup> Na<sub>2</sub>SO<sub>4</sub> + 30 g L<sup>-1</sup> H<sub>3</sub>BO<sub>3</sub> (BS) has been studied by cyclic voltammetry. Boric acid concentration added in the electrolyte solution is the same as of the industrial baths for optimum nickel deposition (pH = 3.5÷4.5). Cyclic voltammograms (CVs) have been recorded on platinum electrode in BS with scan rates between 5 and 500 mV s<sup>-1</sup>.

Kinetic studies of nickel electrodeposition in the absence and presence of different CEFTR concentration, in 25÷65°C temperature range, have been done using linear voltammetry. Linear voltammograms (LVs) were drawn on nickel electrode in 5 g L<sup>-1</sup> Ni<sup>2+</sup> solution (30 g L<sup>-1</sup> H<sub>3</sub>BO<sub>3</sub> + 5 g L<sup>-1</sup> Ni<sup>2+</sup> from NiSO<sub>4</sub>·7H<sub>2</sub>O and NiCl<sub>2</sub>·6H<sub>2</sub>O), with low scan rate (5 mV s<sup>-1</sup>). The activation energy has been determined from Arrhenius plots.

In order to obtain the charge transfer resistance  $R_{ct}$  and surface covering degree  $\theta$ , electrochemical impedance spectroscopy (EIS) has been performed on nickel electrode in the test solutions at different deposition potentials established from LVs. EIS measurements were

carried out in the 0.01 Hz ÷ 100 kHz frequency range with 10 mV AC voltage amplitude. For each spectrum, 60 points were collected with a logarithmic distribution of 10 points per decade. Experimental electrochemical impedance data were fitted to the electrical equivalent circuit by CNLS Levenberg – Marquardt procedure using ZView – Scribner Associates Inc. software.

All solutions have been prepared from Sigma-Aldrich p.a. min. 99.8% reagents. IUPAC name of CEFTR (C<sub>18</sub>H<sub>18</sub>N<sub>8</sub>O<sub>7</sub>S<sub>3</sub>) is (Z)-7-[2-(2-aminothiazol-4-yl)-2-methoxyiminoacetamido]-3-[(2,5-dihydro-6-hydroxy-2-methyl-5-oxo-1,2,4-triazin-3-yl)thiomethyl]-3-cephem-4-carboxylic acid [16], present as disodium salt sesquaterhydrate in the commercial drug Cefort<sup>®</sup>. Its chemical structure is represented in Figure 1 [15]. Concentrations used in experimental studies were 10<sup>-6</sup>, 10<sup>-5</sup>, 10<sup>-4</sup> and 10<sup>-3</sup> mol L<sup>-1</sup>.

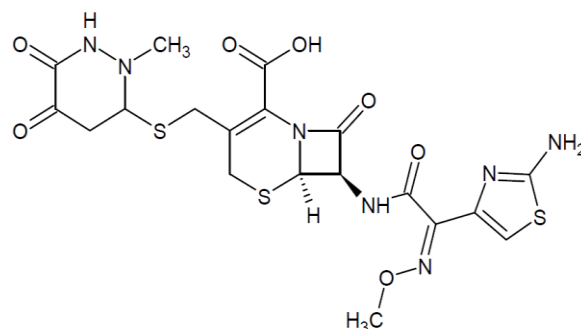


Figure 1. CEFTR chemical structure.

## Results and discussion

### Cyclic voltammetry

Voltammetric behaviour of CEFTR has been studied on platinum electrode at 25°C in BS in the absence and presence of all concentrations of CEFTR used in test solutions. CVs were recorded starting from open circuit potential towards anodic polarization, at scan rates between 500 and 5 mV s<sup>-1</sup>. To ensure a wide potential range for the CV measurements where the electrochemical behaviour was defined, studies have been carried out in electrolyte solutions without nickel ions. CVs drawn with 50 mV s<sup>-1</sup> scan rate are depicted in Figure 2.

The analysis of the above CVs emphasizes the inhibitory effect of CEFTR addition in the electrolyte solutions. It is observed that the increase of CEFTR concentration leads to the current density decrease for the characteristic processes highlighted on the voltammogram drawn in acidic media. Withal, the potential of the hydrogen evolution reaction is shifted towards

more negative values and oxygen evolution reaction toward more positive ones, both processes being inhibited by the presence of CEFTR in the electrolyte solution.

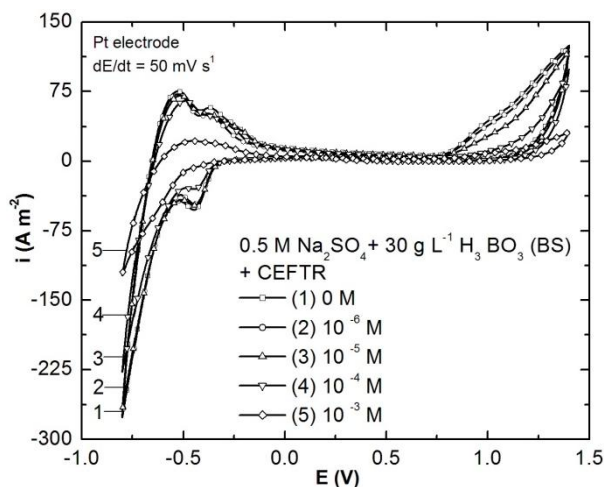


**Figure 2.** CVs (cycle 2) on platinum electrode in BS without and with different concentrations of CEFTR;  $dE/dt = 50 \text{ mV s}^{-1}$ .

At low scan rate,  $5 \text{ mV s}^{-1}$  (Figure 3a), the strong inhibiting influence is observed in the presence of  $10^{-3} \text{ mol L}^{-1}$  CEFTR by the significant decrease of the current density characteristic for hydrogen evolution reaction from  $140$  to  $40 \text{ A m}^{-2}$  and for oxygen evolution reaction from  $40$  to  $10 \text{ A m}^{-2}$ , corresponding to the potential limits of the experimental measurements.

Because nickel electrodeposition is a cathodic process, for a more detailed outlook of CEFTR electrochemical behaviour, CVs on cathodic domain were recorded separately as well (Figure 3b).

Because there cannot be distinguished the supplementary peaks from the base curve characteristic ones, it can be stated that CEFTR does not undergo electrochemical transformations within the studied potential range. Based on this fact, it is expected that CEFTR will be stable during nickel electroplating from Watts bath.

### Linear voltammetry

The effect of CEFTR addition in the electrolyte solutions on nickel electrodeposition has been investigated by LV. LVs were drawn on nickel electrode in  $5 \text{ g L}^{-1} \text{ Ni}^{2+}$  without and with different concentrations of CEFTR in the  $25\div 65^\circ\text{C}$  temperature range (Figure 4).

The analysis of LVs (Figure 4a) pointed out that the temperature increase favours nickel electroplating, the characteristic overpotential being shifted with approximately  $50 \text{ mV}/10^\circ\text{C}$

toward more positive values in the  $25\div 65^\circ\text{C}$  range.

As regards the effect of CEFTR addition in the electrolyte solution at low concentration ( $10^{-6} \text{ mol L}^{-1}$ ) is insignificant compared to the blank solution. In Figure 4c LVs drawn at  $25^\circ\text{C}$  are presented. However, increasing the concentration up to  $10^{-4} \text{ mol L}^{-1}$  leads to the shifting of nickel electrodeposition overpotential with more than  $100 \text{ mV}$  towards more negative values, because of the organic molecule adsorption onto the electrode surface according to Eq.(1).



Accurate information regarding the kinetics of nickel deposition process has been obtained using Tafel method. In Table 1 the values of exchange current density  $i_0$  and cathodic transfer coefficient  $1-\alpha$  are presented, for each concentration of CEFTR used, at all temperatures of the experimental study.

Analysing the results, it can be observed that both in the absence and presence of CEFTR in the electrolyte solution, the rate-determining step is the monoelectronic charge transfer. The catalytic effect of temperature rise on nickel electrodeposition is emphasized by the decrease of the cathodic transfer coefficient  $1-\alpha$  and by the significant increase of exchange current density  $i_0$ .

The cathodic transfer coefficient increases along with CEFTR addition in the electrolyte solution due to the shift of the reaction surface (inner Helmholtz plane) towards the bulk of solution, an obvious effect up to a temperature of  $45^\circ\text{C}$ . At higher temperatures ( $55, 65^\circ\text{C}$ ) it remains almost constant, the blocking effect of active sites with CEFTR being countered by the increase of thermal movement.

Similarly, at lower temperatures ( $25, 35^\circ\text{C}$ ) the exchange current density decreases significantly (about  $10^5$  times) when  $10^{-4} \text{ mol L}^{-1}$  is added in the electrolyte solution, this effect being diminished with the increase of temperature.

Activation energy for nickel deposition in the absence and presence of different concentrations of CEFTR was calculated from the linear dependence:  $\lg i_0 = f(T^{-1})$ . In Figure 5, Arrhenius plots for this process are presented.

For the studied temperature range, where there is a linear dependence  $\lg i_0 = f(T^{-1})$ , activation energy values are a measure of the inhibition effect for nickel deposition due to the adsorption of the organic compound onto the electrode surface.

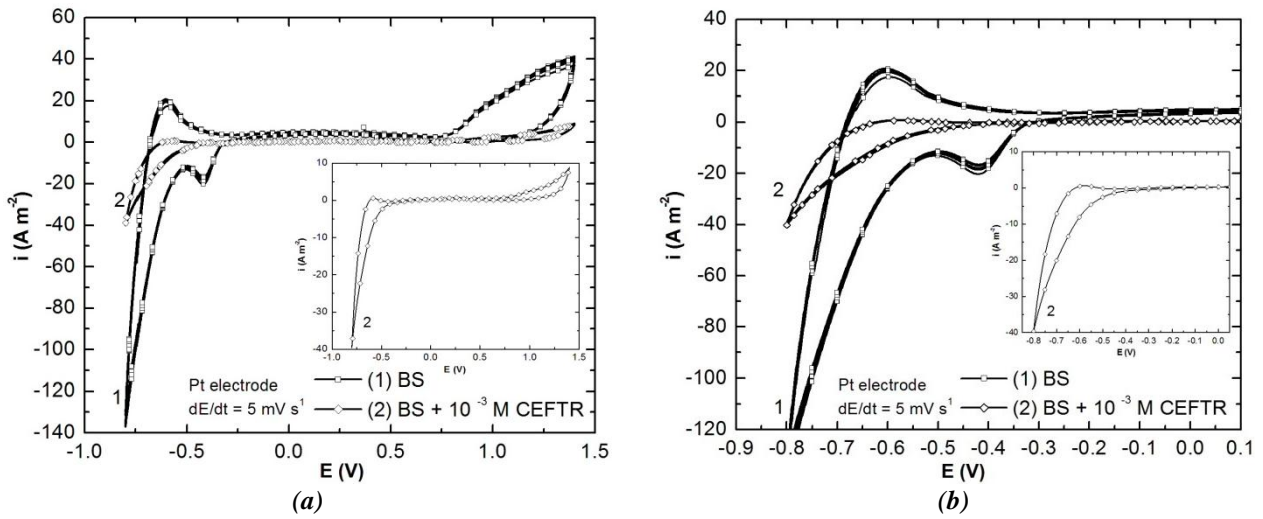


Figure 3. CVs (5 cycles) on platinum electrode in BS and BS with  $10^{-3}$  M CEFTR;  $dE/dt = 5 \text{ mV s}^{-1}$ .

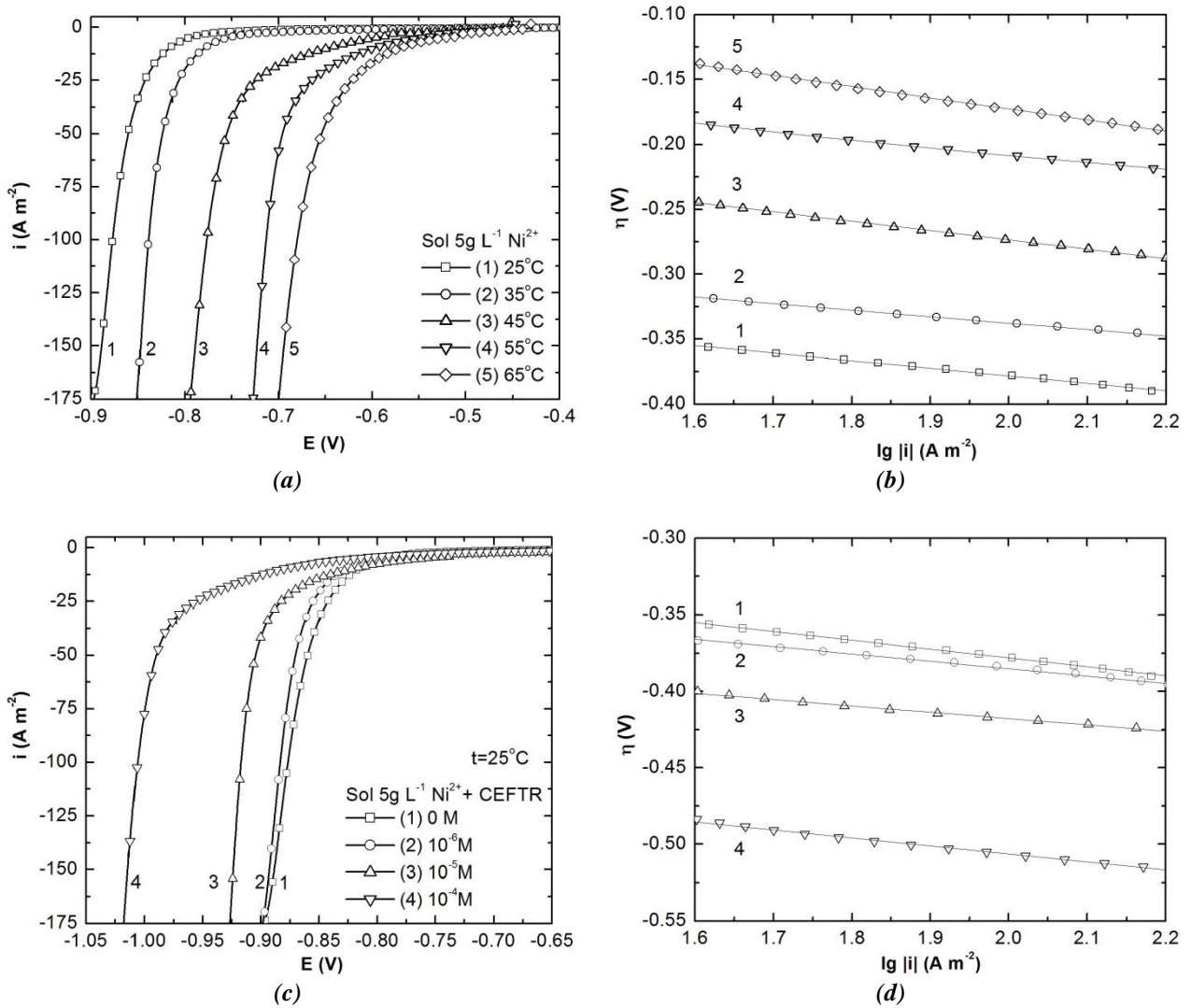


Figure 4. LVs and correspondent Tafel plots on nickel electrode in  $30 \text{ g L}^{-1} \text{ H}_3\text{BO}_3 + 5 \text{ g L}^{-1} \text{ Ni}^{2+}$  at different temperatures (a), (b) and in  $30 \text{ g L}^{-1} \text{ H}_3\text{BO}_3 + 5 \text{ g L}^{-1} \text{ Ni}^{2+}$  without and with different concentrations of CEFTR (c), (d);  $dE/dt = 5 \text{ mV s}^{-1}$ .

In the absence of CEFTR the activation energy is reduced ( $27.2 \text{ kJ mol}^{-1}$ ), but increasing the concentration of organic compound in the electrolyte solution leads to the increase of the activation energy up to  $48.6 \text{ kJ mol}^{-1}$ , when  $10^{-4} \text{ mol L}^{-1}$  is added.

Table 1

**Kinetic parameters for nickel deposition from  $5 \text{ g L}^{-1} \text{ Ni}^{2+}$  solution without and with different concentrations of CEFTR.**

CEFTR conc. ( $\text{mol L}^{-1}$ )	Temperature ( $^{\circ}\text{C}$ )	$1-\alpha$	$i_o$ ( $\text{A m}^{-2}$ )
0	25	0.54	$1.52 \cdot 10^{-5}$
	35	0.52	$2.71 \cdot 10^{-4}$
	45	0.43	$1.02 \cdot 10^{-2}$
	55	0.41	$6.85 \cdot 10^{-2}$
	65	0.39	$6.67 \cdot 10^{-1}$
$10^{-6}$	25	0.55	$8.21 \cdot 10^{-6}$
	35	0.54	$5.18 \cdot 10^{-5}$
	45	0.47	$1.09 \cdot 10^{-3}$
	55	0.41	$9.78 \cdot 10^{-3}$
	65	0.39	$2.87 \cdot 10^{-1}$
$10^{-5}$	25	0.64	$6.70 \cdot 10^{-8}$
	35	0.63	$2.87 \cdot 10^{-6}$
	45	0.49	$1.54 \cdot 10^{-3}$
	55	0.42	$3.87 \cdot 10^{-3}$
	65	0.40	$8.47 \cdot 10^{-2}$
$10^{-4}$	25	0.70	$1.75 \cdot 10^{-10}$
	35	0.64	$8.22 \cdot 10^{-9}$
	45	0.55	$1.83 \cdot 10^{-5}$
	55	0.42	$1.01 \cdot 10^{-3}$
	65	0.40	$1.32 \cdot 10^{-2}$

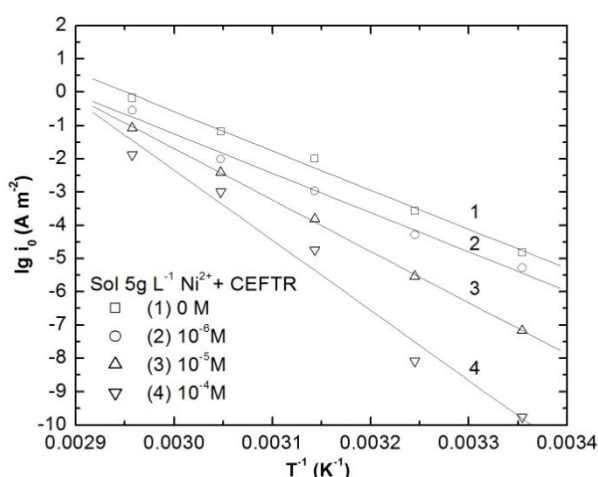


**Figure 5. Arrhenius plots for nickel deposition from  $30 \text{ g L}^{-1} \text{ H}_3\text{BO}_3 + 5 \text{ g L}^{-1} \text{ Ni}^{2+}$  without and with different concentrations of CEFTR.**

### Electrochemical impedance spectroscopy

EIS measurements have been carried out in order to evaluate the charge transfer resistance  $R_{ct}$  and the double layer capacity  $C_{dl}$ , respectively, for a complete characterization of the process occurring at interface. Further, surface coverage degree  $\theta$  has been calculated from  $R_{ct}$  values. Based on the surface coverage degree values, the CEFTR levelling capacity in nickel deposition baths can be anticipated.

Relying on the previously presented LVs, the optimal potential range was chosen, in which nickel deposition is the only process that occurs at the interface ( $-0.5 \div -1.1 \text{ V}$ ).

EIS results expressed as Nyquist plots for nickel electrodeposition from  $5 \text{ g L}^{-1} \text{ Ni}^{2+}$  in the absence and presence of  $10^{-6} \div 10^{-3} \text{ mol L}^{-1}$  CEFTR at  $-0.6 \text{ V}$  are presented in Figure 6.

The shape of Nyquist spectra as a slightly suppressed semicircle indicates an electron transfer limiting process estimated by the charge transfer resistance ( $R_{ct}$ ). The dependence between the diameters of the semicircles and CEFTR concentration added in the electrolyte solution has been observed. The enlargement of the diameters with the increase of the additive concentration proves its inhibitory effect on nickel deposition process.

Figure 7 presents Nyquist (a,b) and Bode (c,d) plots for nickel deposition from  $5 \text{ g L}^{-1} \text{ Ni}^{2+}$  with  $10^{-4} \text{ mol L}^{-1}$  CEFTR, at different potentials.

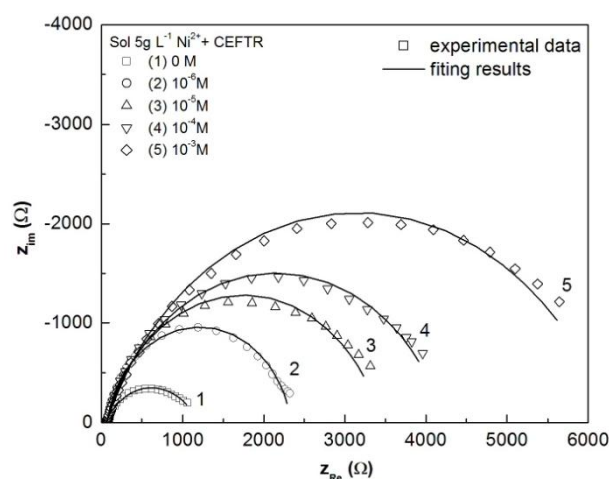


**Figure 6. Nyquist plots recorded on nickel electrode in  $30 \text{ g L}^{-1} \text{ H}_3\text{BO}_3 + 5 \text{ g L}^{-1} \text{ Ni}^{2+}$  without and with different concentrations of CEFTR;  $E = -0.6 \text{ V}$ .**

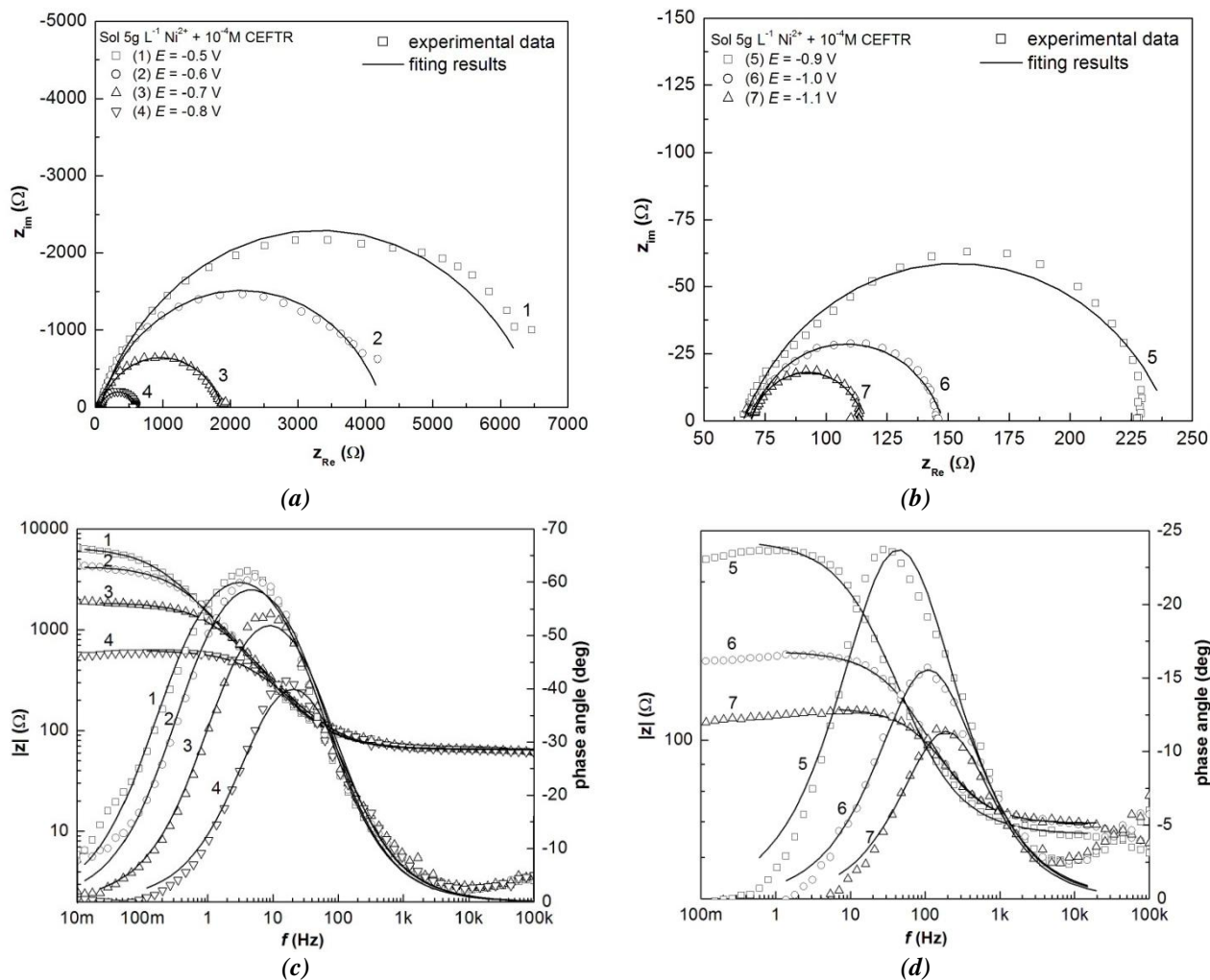


Figure 7. Nyquist (a), (b) and Bode plots (c), (d) recorded on nickel electrode in 30 g L<sup>-1</sup> H<sub>3</sub>BO<sub>3</sub>+5 g L<sup>-1</sup> Ni<sup>2+</sup> with 10<sup>-4</sup> M CEFTR at different potentials.

Experimental data have been fitted to the electrical equivalent circuit (Figure 8) consisting of an ohmic resistance ( $R_s$ ) connected in series with a parallel connection between the charge transfer resistance ( $R_{ct}$ ) and double layer capacity (CPE), using a complex non-linear least squares procedure.

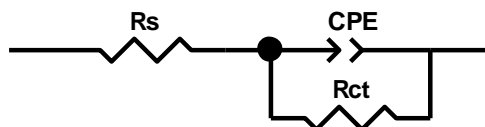


Figure 8. Equivalent electrical circuit for modelling nickel electrodeposition.

Calculated data of the circuit elements on Ni in 5 g L<sup>-1</sup> Ni<sup>2+</sup> without and with various concentrations of CEFTR and surface coverage degree values are presented in Table 2. From the results presented in Table 2 it can be stated that the solution resistance  $R_s$  remains constant within reasonable limits. The charge transfer resistance  $R_{ct}$  is decreasing when the deposition overpotential is shifted towards negative values. At the same potential values,  $R_{ct}$  increases along with CEFTR concentration in the electrolyte solution, thus confirming the results obtained by LV. CEFTR strong adsorption at the interface is demonstrated by the decrease of a double layer capacity  $C_{dl}$  when CEFTR is added in the electrolyte solution. Surface coverage degree  $\theta$  values for CEFTR concentrations over 10<sup>-5</sup> mol L<sup>-1</sup> show a high levelling capacity. Consequently, it is possible to obtain metallic deposits having microcrystalline structure.

Table 2

Calculated data of the circuit elements and experimental errors (between brackets).									
CEFTR conc. (mol L <sup>-1</sup> )	E (V)	R <sub>s</sub> (Ω cm <sup>2</sup> )	T·10 <sup>5</sup> (F cm <sup>-2</sup> s <sup>n-1</sup> )	n	R <sub>ct</sub> (Ω cm <sup>2</sup> )	C <sub>d</sub> ·10 <sup>5</sup> (F cm <sup>-2</sup> )	Chi <sup>2</sup> ·10 <sup>3</sup>	θ (%)	
0	-0.5	54.1 (0.76 %)	56.4 (2.00 %)	0.84 (0.75 %)	2670 (1.64 %)	60.02	11.5	-	
	-0.6	53.6 (0.68 %)	44.3 (2.11 %)	0.85 (0.78 %)	1627 (1.73 %)	41.82	8.7	-	
	-0.7	53.3 (0.75 %)	41.8 (2.66 %)	0.86 (0.93 %)	881 (1.67 %)	35.71	10.1	-	
	-0.8	53.9 (0.57 %)	31.2 (2.70 %)	0.87 (0.80 %)	613 (0.99 %)	24.43	7.3	-	
	-0.9	54.1 (0.18 %)	18.4 (4.21 %)	0.89 (0.81 %)	31 (0.52 %)	9.88	2.2	-	
	-1.0	55.3 (0.16 %)	7.5 (6.19 %)	0.91 (0.96 %)	14 (0.65 %)	3.81	3.1	-	
	-1.1	54.8 (0.14 %)	5.4 (8.45 %)	0.93 (1.18 %)	10 (0.80 %)	3.05	6.0	-	
10 <sup>-6</sup>	-0.5	66.5 (0.63 %)	52.2 (1.00 %)	0.83 (0.42 %)	3585 (1.73 %)	59.14	13.3	25.52	
	-0.6	70.1 (0.33 %)	42.0 (1.05 %)	0.84 (0.28 %)	2268 (0.58 %)	41.61	3.1	28.26	
	-0.7	66.1 (0.53 %)	34.3 (1.52 %)	0.85 (0.57 %)	1248 (1.82 %)	29.51	10.0	29.41	
	-0.8	65.5 (0.41 %)	26.0 (1.62 %)	0.85 (0.51 %)	881 (0.95 %)	20.07	5.4	30.43	
	-0.9	64.5 (0.17 %)	17.8 (4.74 %)	0.86 (0.92 %)	45 (0.60 %)	8.18	3.0	31.11	
	-1.0	65.9 (0.13 %)	7.8 (6.88 %)	0.89 (1.07 %)	21 (0.77 %)	3.65	2.0	32.43	
	-1.1	67.2 (0.09 %)	6.2 (7.01 %)	0.92 (1.01 %)	14 (0.73 %)	3.41	1.4	34.07	
10 <sup>-5</sup>	-0.5	70.4 (0.39 %)	46.4 (0.84 %)	0.80 (0.25 %)	4878 (0.79 %)	56.96	4.3	45.26	
	-0.6	66.2 (0.57 %)	37.4 (1.19 %)	0.83 (0.49 %)	3068 (1.29 %)	38.50	11.9	46.97	
	-0.7	70.0 (0.24 %)	23.2 (1.32 %)	0.83 (0.30 %)	1683 (0.38 %)	19.15	1.9	47.65	
	-0.8	69.6 (0.22 %)	18.1 (2.87 %)	0.86 (0.59 %)	1204 (0.63 %)	14.16	1.8	49.09	
	-0.9	71.9 (0.14 %)	15.5 (4.77 %)	0.87 (0.85 %)	63 (0.74 %)	7.59	1.1	50.79	
	-1.0	67.5 (0.14 %)	12.3 (7.47 %)	0.87 (1.25 %)	29 (0.97 %)	5.32	1.4	51.72	
	-1.1	71.0 (0.14 %)	8.2 (11.48 %)	0.89 (1.72 %)	20 (1.32 %)	3.83	2.3	52.50	
10 <sup>-4</sup>	-0.5	65.6 (0.77 %)	14.9 (1.50 %)	0.75 (0.51 %)	6511 (1.45 %)	14.80	9.6	58.99	
	-0.6	65.6 (0.81 %)	13.1 (1.85 %)	0.77 (0.58 %)	4010 (1.33 %)	10.85	11.3	59.43	
	-0.7	65.6 (0.82 %)	12.4 (2.52 %)	0.77 (0.71 %)	2212 (1.24 %)	8.40	11.5	60.17	
	-0.8	64.5 (0.76 %)	11.5 (3.97 %)	0.78 (0.98 %)	1584 (1.31 %)	7.13	10.6	61.30	
	-0.9	66.0 (0.63 %)	10.9 (5.24 %)	0.79 (1.22 %)	85 (1.24 %)	3.20	3.1	63.53	
	-1.0	69.1 (0.35 %)	9.9 (5.15 %)	0.80 (0.01 %)	41 (0.85 %)	2.51	1.2	65.85	
	-1.1	69.4 (0.44 %)	6.8 (11.23 %)	0.82 (1.92 %)	28 (1.77 %)	1.71	2.6	66.07	
10 <sup>-3</sup>	-0.5	65.0 (0.69 %)	9.1 (1.18 %)	0.72 (0.37 %)	10049 (1.11 %)	8.81	3.5	73.43	
	-0.6	65.8 (0.48 %)	8.2 (1.07 %)	0.74 (0.31 %)	6322 (0.85 %)	6.51	2.5	74.26	
	-0.7	66.2 (0.34 %)	7.2 (0.97 %)	0.75 (0.25 %)	3528 (0.42 %)	4.59	1.1	75.03	
	-0.8	67.8 (0.19 %)	6.2 (0.94 %)	0.75 (0.21 %)	2584 (0.26 %)	3.39	0.6	76.28	
	-0.9	68.3 (0.34 %)	5.4 (2.26 %)	0.77 (0.61 %)	144 (0.58 %)	1.26	2.0	78.47	
	-1.0	72.0 (0.35 %)	4.1 (3.46 %)	0.78 (0.92 %)	72 (0.67 %)	0.81	2.4	80.56	
	-1.1	72.5 (0.17 %)	3.6 (3.06 %)	0.79 (0.70 %)	54 (0.44 %)	0.67	1.1	82.41	

## Conclusions

Cyclic voltammetry curves have revealed that CEFTR does not undergo electrochemical transformations, but strongly inhibit both cathodic and anodic processes (hydrogen and oxygen evolution reactions, respectively) meaning CEFTR is stable in the Watts baths.

Linear voltammograms have demonstrated that CEFTR has a strong inhibitory effect on nickel electrodeposition. Whether CEFTR addition in Ni<sup>2+</sup> solution increases the cathodic transfer coefficient 1-α with the increase of the inhibitor concentration, the overall process is given by the significant decrease of exchange current density *i*<sub>0</sub>. For instance, when

10<sup>-4</sup> mol L<sup>-1</sup> CEFTR is added in 5 g L<sup>-1</sup> Ni<sup>2+</sup>, *i*<sub>0</sub> decreases about 10<sup>5</sup> times.

Overall effect of CEFTR addition on nickel deposition has been illustrated in detail by the activation energy, which increases from 27.2 kJ mol<sup>-1</sup> in the electrolyte solution without additive to 48.7 kJ mol<sup>-1</sup> in the solution with 10<sup>-4</sup> mol L<sup>-1</sup> CEFTR.

Electrochemical impedance spectroscopy data have confirmed the conclusions reached from the CV and LV measurements. From the experimental data, CEFTR from expired Cefort<sup>®</sup> drug should be recommended as an additive in nickel electroplating Watts baths.

## Acknowledgment

This work was partially supported by University Politehnica Timisoara in the frame of PhD studies.

## References

1. Muhammad, R.A.; Uday, M.B.; Alias, M.N.; Norhayati, A.; Srithar, R. Microstructural evaluation of a slurry based Ni/YSZ thermal barrier coating for automotive turbocharger turbine application. *Materials and Design*, 2016, 109, pp. 47–56. DOI: [10.1016/j.matdes.2016.07.070](https://doi.org/10.1016/j.matdes.2016.07.070).
2. Lv, B.; Hu, Z.; Wang, X.; Xu, B. Electrodeposition of nanocrystalline nickel assisted by flexible friction from an additive-free Watts bath. *Surface and Coatings Technology*, 2015, 270, pp. 123–131. DOI: [10.1016/j.surfcoat.2015.03.012](https://doi.org/10.1016/j.surfcoat.2015.03.012).
3. Abdallah, M.; El-Etre, A-Y. Corrosion inhibition of nickel in sulfuric acid using tween surfactants. *Portugaliae Electrochimica Acta*, 2003, 21, pp. 315–326.
4. Fouda, A.S.; Tawfik, H.; Abdallah, N.M.; Ahmd, A.M. Corrosion inhibition of nickel in HCl solution by some indole derivatives. *International Journal of Electrochemical Science*, 2013, 8, pp. 3390–3405.
5. Chianpairot, A.; Lothongkum, G.; Schuh, C.A. Corrosion of nanocrystalline Ni–W alloys in alkaline and acidic 3.5 wt.% NaCl solutions. *Corrosion Science*, 2011, 53, pp. 1066–1071.
6. Rudnik, E.; Wojnicki, M.; Wloch, G. Effect of gluconate addition on the electrodeposition of nickel from acidic baths. *Surface and Coatings Technology*, 2012, 207, pp. 375–388. DOI: [10.1016/j.corsci.2010.12.001](https://doi.org/10.1016/j.corsci.2010.12.001).
7. Oliveira, E.M.; Finazzi, G.A.; Carlos, I.A. Influence of glycerol, mannitol and sorbitol on electrodeposition of nickel from a Watts bath and on the nickel film morphology. *Surface and Coatings Technology*, 2006, 200, pp. 5978–5985.
8. Rashidi, A.M.; Amadeh, A. The effect of saccharin addition and bath temperature on the grain size of nanocrystalline nickel coatings. *Surface and Coatings Technology*, 2009, 204, pp. 353–358. <https://doi.org/10.1016/j.surfcoat.2009.07.036>.
9. Mosavat, S.H.; Bahrololoom, M.E.; Shariat, M.H. Electrodeposition of nanocrystalline Zn–Ni alloy from alkaline glycinate bath containing saccharin as additive. *Applied Surface Science*, 2011, 257, pp. 8311–8316. <https://doi.org/10.1016/j.apsusc.2011.03.017>.
10. Sakamoto, T.; Azumi, K.; Tachikawa, H.; Iokibe, K.; Seo, M.; Uchida, N. Effects of 2-buthyne-1,4-diol additive on electrodeposited Ni films from a Watts-type bath. *Electrochimica Acta*, 2010, 55, pp. 8570–8578. DOI: <https://doi.org/10.1016/j.electacta.2010.07.031>.
11. Schlesinger, M.; Paunovic, M. Eds. *Modern Electroplating* 5th edition. Wiley: New Jersey, 2010, pp.79–114.
12. Duca, D.A.; Vaszilcsin, N.; Dan, M.L. Recycling of expired midazolam as levelling agent in a Watts electroplating bath. *SGEM2016 Conference Proceedings*, 2016, 4(2), pp. 105–112.
13. Kozak, M.A.; Melton, J.R.; Gernant, S.A.; Snyder, M.E. A needs assessment of unused and expired medication disposal practices. *Research in Social and Administrative Pharmacy*, 2015, 12(2), pp 336–340. DOI: [10.1016/j.sapharm.2015.05.013](https://doi.org/10.1016/j.sapharm.2015.05.013).
14. Tong, A.Y.C.; Peake, B.M.; Braund R. Disposal practices for unused medications around the world. *Environment International*, 2011, 37, pp. 292–298. DOI: <https://doi.org/10.1016/j.envint.2010.10.002>.
15. Duca, D.A.; Dan, M.L.; Vaszilcsin N. Reuse of expired cefort drug in copper electrodeposition from acid bath. *Annals of University of Oradea, Fascicle Environmental Protection*, 2016, 27, pp. 229–236.
16. Parfitt, K. Ed. *The complete drug reference*. 32<sup>nd</sup> edition. Pharmaceutical Press: London, 1999, 176 p.